Equations of state of six metals above 94 GPa

Agnès Dewaele,[1] Paul Loubeyre,[1] and Mohamed Mezouar[2]
[1]*DIF/Département de Physique Théorique et Appliquée, CEA, BP 12, 91680 Bruyères-le-Châtel, France*
[2]*European Synchrotron Radiation Facility, BP 220, F-38043 Grenoble Cedex, France*
(Received 17 March 2004; revised manuscript received 3 June 2004; published 22 September 2004)

Compression versus pressure at ambient temperature has been measured for tantalum, gold, and platinum to 94 GPa and for aluminum, copper, and tungsten to 153 GPa, in a diamond anvil cell. Standard synchrotron x-ray diffraction accuracy in the volume determination could be achieved to the maximum pressure. The current data set is used to recalibrate the static pressure scale based on the ruby luminescence, confirming recent suggestions of an underestimation of pressure. Using an updated pressure calibration, the consistency between ultrasonic, dynamic, and static measurements of the equations of state is improved for these six equations of state. This consistency allows us to test the predictive power of density functional theory, with different approximations, for equation-of-state calculations. For example, the generalized gradient approximation leads to very accurate results, except for gold, the heaviest element.

DOI: 10.1103/PhysRevB.70.094112 PACS number(s): 64.30.+t, 07.35.+k, 71.15.Nc

I. INTRODUCTION

Recently, important advances have been achieved in static high-pressure experiments. Not only has the pressure-temperature range of measurements been significantly extended but it has also been shown that the measurements could be performed under these extreme conditions with almost similar accuracy to ambient pressure.[1–3] In particular, using the x-ray beam of the third generation synchrotrons, single-crystal x-ray diffraction (XRD) could be extended in the Mbar range, even for the lightest systems, and subtle changes detected.[4,5] The joint use of helium as a quasihydrostatic pressure medium and tiny crystal samples helped to prevent measurement biases due to the deviatoric stress and hence to reach the actual thermodynamic state.

However, the absolute accuracy of these equation-of-state (EOS) measurements cannot be higher than the accuracy of the static pressure scale. Unlike for shock-wave experiments, the pressure cannot be directly measured in static experiments. Therefore, secondary pressure scales must be used, such as luminescence gauges,[6,7] and x-ray gauges.[8,9] At ambient temperature, the ruby luminescence pressure scale is the most widely used. It has been calibrated using shock-wave equations of state, reduced to ambient temperature (RSW-EOS), of Ag, Cu, Pd, and Mo up to 80 GPa.[6,10] Recently, an absolute calibration of the ruby scale has been established up to 55 GPa.[11] This study has verified that the ruby scale was accurate within 2% up to 55 GPa. This has also shown that the method of using the volume of metals as primary standards is suitable to calibrate the ruby pressure scale. But recent analyses of the static EOS data of diamond and Ta have suggested that the ruby pressure scale could underestimate pressure by $\simeq$10 GPa at 150 GPa.[12–14]

The first aim of the present study is to extend the calibration of the ruby gauge up to higher pressure, following the method developed by Mao *et al.*,[10] but with higher precision in the volume determination of the metals and by taking into account recent studies on the robustness of the reduction of shock-wave data. Six metals were chosen for this calibration: on the one hand, Al [$Z=13$; $[Ne]3s^23p$; face-centered-cubic (fcc) structure], Cu ($Z=29$; $[Ar]3d^{10}4s$; fcc structure), Ta ($Z=73$; $[Xe]4f^{14}5d^36s^2$; body-centered-cubic (bcc) structure), *W* ($Z=74$; $[Xe]4f^{14}5d^46s^2$; bcc structure) because they have been extensively studied by dynamic compression; on the other hand, Pt ($Z=78$; $[Xe]4f^{14}5d^96s$; fcc structure), and Au ($Z=79$; $[Xe]4f^{14}5d^{10}6s$; fcc structure) because they are often used as x-ray pressure gauges. Also, all these metals keep their simple structures to the maximum pressure studied.

The second aim of the present study, subsequent to the first aim, is to constitute an accurate data set of the EOS of metals, with simple structures, no phase transition and spanning a large range of values of the electronic number (from $Z=13$ to 79), so as to be able to reliably test electronic structure calculations. Density functional electronic structure (DFT) calculations are now widely used to calculate the cohesive energy of solids versus volume and its derivative, the EOS, but DFT calculations rest on approximations [e.g., local density approximation (LDA) or generalized gradient approximation (GGA)] and their validity is established by the ability to reproduce experimental data. The LDA and GGA have been found to produce pressures that provide, respectively, lower bounds and upper bounds to the observed pressure for a given volume.[15] In the present study we want to quantify this deviation over a significant compression range.

II. EXPERIMENTAL METHOD AND DATA

Five experiments have been performed with the same sample geometry. Three crystal grains (4 μm in the maximum dimension), respectively of tungsten, copper, and aluminum in two runs, and tantalum, platinum, and gold in three runs have been loaded in a membrane diamond anvil cell with a large x-ray aperture, ensured by the use use of boron diamond supports. All metal crystals have been selected from commercial powders (purity from 99.8% to 99.95%). Helium was the pressure transmitting medium. The pressure was estimated from the pressure calibration of the luminescence of a 4-μm ruby ball.[6] The ruby ball was placed touching the

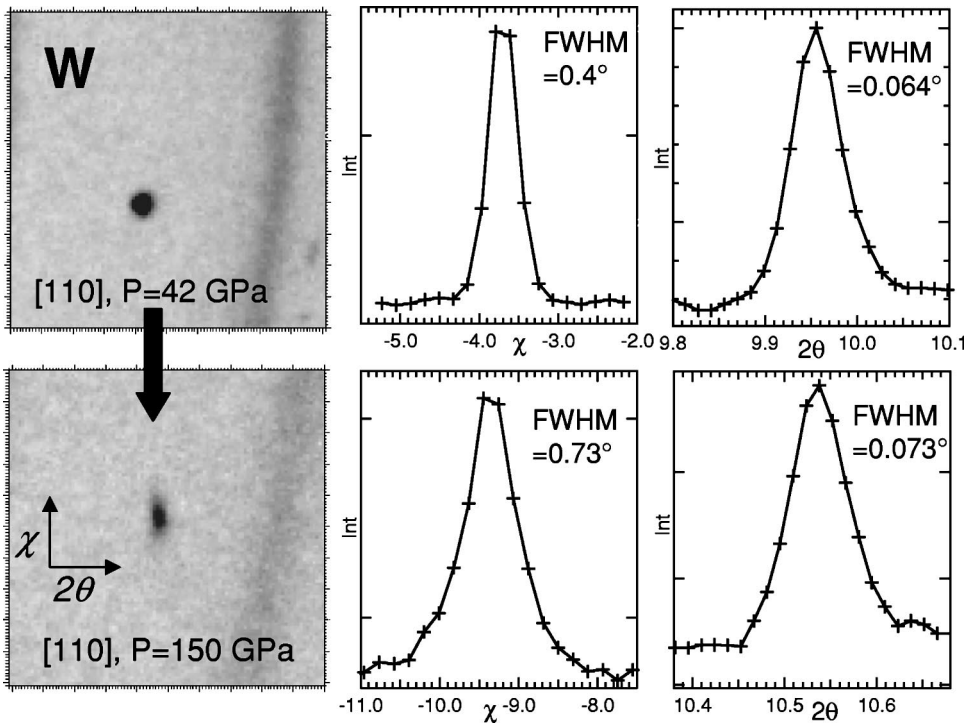

FIG. 1. (left) [110] diffraction peak of a tungsten single crystal, recorded on an imaging plate while rotating the diamond anvil cell by ±15° around a vertical axis, at 42 and 150 GPa. (middle) Same peak after integration in 2θ (the diffraction angle); at 150 GPa, the diffraction peak appears slightly broadened in azimuthal angle (χ). (right) Same peak after integration in χ. In 2θ, broadening is very weak (from 0.064° full width at half maximum at the beginning of the experiment to 0.073° at 150 GPa). These spectra evidence a slight increase of the mosaicity of the sample at very high pressure and qualitatively show the quasihydrostatic conditions of the helium pressure transmitting medium.

metals crystal grains at the center of the sample chamber. The pressure error bars range from 0.05 GPa at 1 GPa to 2 GPa at 150 GPa, if the ruby pressure scale is assumed to be correct. The lattice parameters of these metals have been measured by angle dispersive monochromatic ($\lambda = 0.3738$ Å) XRD technique at the ESRF. The diffracted signal has been recorded on a MARE3450 imaging plate system, located at a distance of $\simeq$400 mm from the sample. The diffraction geometry was determined using a Silicium reference sample. Maximum 2θ value was 23°. Diffracted signal showed that the metal grains had different microstructures. The tantalum, tungsten, and aluminum grains were single crystals, while the platinum, copper, and gold grains were fine powders. Diffraction images were scanned with 100 μm spatial resolution and integrated using the Fit2D software.[16] Powder spectra have been analyzed using Datlab and the lattice parameter optimized taking into account all diffracted peaks. Single-crystal diffracted peaks (number ranging from 4 for aluminum to 12 for tungsten) were individually integrated after refinement of the beam center. No evidence of nonhydrostatic compression could be evidenced with these two analysis, the relative differences between apparent lattice parameters for different Bragg peaks remaining smaller than 5×10^{-4} in the worst case, Al. In all cases, the relative uncertainty in the lattice parameters was smaller than 10^{-3}. We checked by interferometry that the thickness of the sample chamber was always larger than the dimension of the crystals, to ensure that samples were not bridged between diamonds. Neither the ruby fluorescence spectra nor the values of measured interreticular distances exhibited any evidence of nonhydrostatic stresses up to 150 GPa. Furthermore, as shown in Fig. 1, the degradation of tungsten single-crystal diffraction peaks upon pressure increase was weak, suggesting qualitatively that nonhydrostatic stresses remained small. Reference zero-pressure spectra have been recorded at the end of two runs, for all studied metals, after decompression and with the same samples and diffraction geometry as low-pressure points.

The lattice parameters of the six metals measured up to 144 GPa are presented in Fig. 2. Corresponding atomic volumes are listed in Table I. The scatter of the data remains within ±0.02 Å^3, except for Al. For that element, the diffracted signal was very weak. This scatter can be assigned to the intrinsic precision of angle dispersive XRD technique. For each metal, the $P(V)$ data have been fitted with a Vinet formulation of the EOS.[17] This provides three parameters that characterize an EOS—namely, the volume V_0, the bulk modulus K_0, and its pressure derivative K_0' at ambient pressure. It is important to reach sufficient compression ($\simeq$20% in volume) to constrain the K_0' value. For all studied metals, V_0 has been deduced from the low-pressure measurements ($0 \leqslant P \leqslant 5$ GPa), leading to values which agree with literature[18,19] within 10^{-3}. The value of V_0 was then fixed during the whole data set fitting. It was possible to fit the experimental data with either K_0 and K_0' treated as free parameters or by fixing K_0 to its ultrasonic value, without any major decrease of the fit quality. The fitting results are presented in Table II. Gold and platinum EOS compare correctly with previous measurements, carried out at lower pressures.[28,29] Aluminum, tungsten, and tantalum EOS data exhibit much less scatter than previous XRD determinations,[30–33] and consequently lead to EOS parameters that are better constrained.

III. COMPARISON WITH OTHER EXPERIMENTAL DATA: IMPLICATIONS FOR THE RUBY PRESSURE CALIBRATION

To test static high-pressure metrology, the XRD EOS of these metals must be compared to the EOS obtained from the

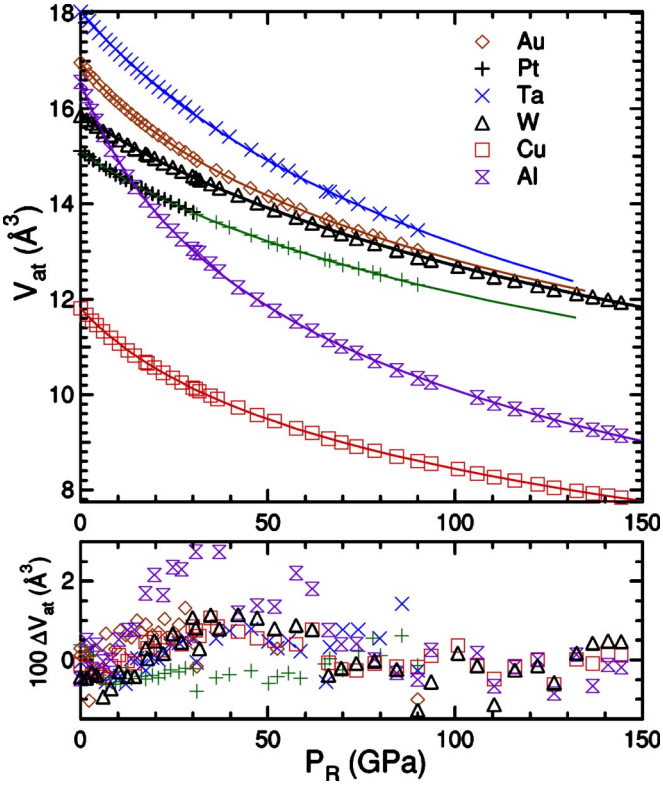

FIG. 2. Evolution of the atomic volume of the six metals versus pressure. The pressure is measured with the ruby scale. The symbols are the data points and the lines are the fit of the data obtained with the Vinet formulation of the EOS (Ref. 17): $P=3K_0x^{-2}(1-x)\exp[(1.5K_0'-1.5)(1-x)]$. The parameters of this formulation are V_0, volume, K_0, bulk modulus, and K_0', its pressure derivative, under ambient conditions $[x=(V/V_0)^{1/3}]$. The values of fitted parameters for each metal are presented in the third column of Table II. The difference between the data points and the fits is presented in the lower part of the figure.

reduction of shock wave data to 298 K. In dynamic compression experiments, shock velocity and particle velocity are measured during the shock. Then, the pressure P, the volume V, and the internal energy are calculated using the Rankine-Hugoniot relations.[34] The temperature in shocked metals typically reaches 5000 K at 200 GPa. The P-V shock data are then generally reduced to ambient temperature, in a quasiharmonic framework,[25] using the Mie-Grneisen formalism. Fully *ab initio* reductions have also been carried out recently,[23] using a mean-field potential approach, which are in good agreement with empirical reductions.

In Table II, we have listed the parameters of the RSW-EOS of Au, Pt, Ta, W, Cu, and Al obtained by the most recent works. For all metals, the RSW-EOS have been fitted by the Vinet EOS between 0 and 160 GPa to obtain the parameters K_0 and K_0'. There is consensus on the experimental Hugoniot curve of copper up to 200 GPa[34–36]. This metal thus appears to be a good pressure calibrant in our pressure range. On the contrary, we found discrepancies between recently published Pt and Au RSW-EOS[8,23] and previous works.[37,38]

The comparison between the RSW-EOS and our x-ray diffraction measurements is presented in Fig. 3(a). At high pressure, all shock wave pressures become larger than the ruby pressure. This could be explained by nonhydrostatic effects in the previous ruby pressure calibration experiment,[6] carried out with argon as pressure medium. In fact, the RSW-EOS used for copper in Ref. 6 is the same as in the present study, and consequently, the difference between the two calibrations must be ascribed to the difference between the static EOS data. Qualitatively, if the volume is overestimated by x rays, as expected in a nonhydrostatic experiment, pressure will be underestimated by the use of an hydrostatic RSW-EOS, which is the trend observed in Fig. 3(a). We believe that the use of several metals that have been independently studied by shock waves, including one on which there is an experimental consensus (Cu), prevents us from a major bias due to a wrong RSW-EOS. We thus conclude that the ruby pressure scale[6] underestimates the pressure, especially above 100 GPa. This is new strong experimental evidence that supports earlier doubts about the ruby pressure calibration[12–14]. We propose a simple modification of this scale that minimizes differences with all RSW-EOS plotted in Fig. 3. If the same simple algebric form as the one of Ref. 6 is kept,

$$P_R' = A/B[(\lambda/\lambda_0)^B - 1], \tag{1}$$

with the same low-pressure dependence ($A=1904$ GPa), a value of $B=9.5$ (instead of 7.665) reconciles the current XRD EOS and RSW-EOS over the pressure range investigated. This is shown in Fig. 3(b), where no systematic trend is observed in $P_{SW}-P_R'$. Since all x-ray diffraction EOS have been established using the same pressure scale, the ruby scale, the dispersion between the various curves in Fig. 3(b) also yields an estimate of the uncertainty in RSW-EOS, even if this uncertainty is not absolute. Au and Pt curves are, respectively, the lowest and highest; uncertainties in these RSW-EOS may thus be larger than for other studied metals. When these two metals are used as pressure calibrants, the current static EOS may be used preferably to the RSW-EOS previously published.[23] The present ruby scale calibration nearly follows the copper RSW-EOS, on which there is a consensus and for which the absolute error bars should be the smallest.

The difference between P_R and P_R' plotted in Fig. 4 is smaller than 2% below 55 GPa, which is compatible with the recent conclusion of an absolute calibration of the pressure scale.[11] The correction that has been recently proposed by two authors,[12,13] also plotted in Fig. 4, falls within estimated error bars of the current calibration ($\simeq\pm3$ GPa at 150 GPa). With the present data, we cannot find any clear evidence that the pressure correction should be negative at $P<30$ GPa, as proposed by Holzapfel; however, this possibility cannot be ruled out. More compressible materials should be studied for that purpose.

With the new ruby calibration (P_R'), new values of K_0 and K_0' of the EOS of the six studied metals have been obtained. A decrease of bulk modulus in the reference state K_0 (1–3 GPa) and an increase of its pressure derivative K_0' (0.3–0.4) is obtained, which leads to parameters closer to the parameters deduced from acoustic data (see Table II). In Table II, it is encouraging to see that the three different ex-

TABLE I. Atomic volumes of Cu, W, Al and Au, Pt, Ta, measured by angle-dispersive x-ray diffraction, with helium pressure transmitting medium, as a function of the ruby luminescence pressure. P_R is the pressure obtained from the "classical" calibration (Ref. 6) and P'_R from the current calibration [Eq. (1), with $A=1904$ GPa and $B=9.5$]. Experimental uncertainty in V is 0.01 Å^3/at. Uncertainty in P_R increases from 0.05 GPa at 1 GPa to 2 GPa at 150 GPa, if the ruby pressure scale is assumed to be correct.

First two runs					Last three runs				
P_R (GPa)	P'_R (GPa)	Cu V (Å^3/at)	W V (Å^3/at)	Al V (Å^3/at)	P_R (GPa)	P'_R (GPa)	Au V (Å^3/at)	Pt V (Å^3/at)	Ta V (Å^3/at)
1.53	1.53	11.675	15.770	16.257	2.27	2.27	16.716	14.979	17.838
3	3.01	11.551	15.698	15.952	3.43	3.44	16.642	14.921	17.704
4.25	4.26	11.458	15.632	15.743	4.99	5.0	16.494	14.830	17.585
6	6.02	11.328	15.532	15.443	6.74	6.76	16.373	14.741	17.436
8.05	8.08	11.196	15.439	15.136	7.84	7.87	16.276	14.693	17.354
10.2	10.3	11.068	15.349	14.855	9.24	9.28	16.170	14.625	17.243
12.5	12.6	10.929	15.243	14.575	10.59	10.6	16.084	14.566	17.140
14.4	14.5	10.822	15.160	14.358	12.04	12.1	15.979	14.509	17.026
17.3	17.4	10.684	15.054	14.076	13.49	13.6	15.880	14.442	16.942
19.7	19.9	10.570	14.961	13.855	15.04	15.2	15.790		16.833
22	22.2	10.457	14.861	13.636	16.14	16.3	15.714	14.334	16.751
24.6	24.9	10.352	14.773	13.436	17.39	17.5	15.642	14.281	16.662
26.9	27.2	10.253	14.681	13.255	19.14	19.3	15.532	14.215	16.557
29.9	30.3	10.146	14.587	13.056	20.79	21.0	15.440	14.149	16.449
31.7	32.2	10.073	14.503	12.971	22.39	22.6	15.361	14.092	16.353
34.7	35.3	9.977	14.421	12.748	23.99	24.3	15.263	14.035	16.263
0	0	11.808	15.852	16.561	26.24	26.6	15.157	13.952	16.129
17.8	18	10.656	15.027		27.89	28.3	15.087	13.897	16.036
30.7	31.1	10.114	14.552	12.989	30.05	30.5	14.961	13.822	15.914
37	37.1	9.909	14.334	12.580	1.14	1.14	16.852	15.044	17.933
42	42.8	9.729	14.182	12.253	0	0	16.966	15.105	18.034
47.1	48.1	9.573	14.022	11.990	52.5	53.8	14.079	13.146	14.814
51.8	53	9.442	13.877	11.763	58.7	60.3	13.881	12.985	14.554
57.5	59	9.293	13.718	11.531	65.5	67.4	13.679	12.837	14.266
61.8	63.5	9.198	13.600	11.344	70.0	72.2	13.542	12.721	14.143
66.2	68.2	9.076	13.456	11.148	78.0	80.7	13.339	12.566	
69.6	71.8	8.997	13.375	11.014	90.0	93.6	13.030	12.305	13.449
73.6	76	8.913	13.280	10.874	31.0	31.5	14.903	13.776	15.843
78.5	81.3	8.819	13.166	10.702	36.2	36.8	14.709	13.616	15.585
84.4	87.6	8.705	13.027	10.509	39.5	40.2	14.564	13.510	15.415
90	93.6	8.603	12.878	10.342	45.3	46.2	14.332	13.342	15.135
93.6	97.5	8.549	12.821	10.261	50.2	51.4	14.159	13.204	14.919
100.7	105.0	8.439	12.694		55.3	56.8	13.990	13.073	14.693
105.9	111.0	8.345	12.584	9.942	66.5	68.5	13.635	12.809	14.257
110.4	116.0	8.270	12.473	9.814	74.1	76.6	13.430	12.639	13.998
115.9	122.0	8.197	12.394	9.702	79.9	82.8	13.278	12.512	13.795
122	128.0	8.118	12.288	9.574	85.7	89.0	13.160	12.408	13.633
126.4	133.0	8.044	12.201	9.461					
132.4	140.0	7.984	12.118	9.366					
136.7	145.0	7.928	12.055	9.264					
140.8	149.0	7.885	11.990	9.201					
144.3	153.0	7.843	11.936	9.136					

TABLE II. Parameters of the Vinet EOS obtained by a least-squares fit of the experimental data, with the pressure scale of Ref. 6 (P_R) and our pressure scale (P'_R). the bold values have been fixed during the fitting procedure. Numbers between parentheses are the fitting error bars (95% confidence interval) on the last or the two last digits. For comparison, RSW-EOS (reduced shock-wave equation of state) parameters, determined by fitting of RSW-EOS by the Vinet EOS between 0 and 160 GPa, and acoustic values of K_0 and K'_0 have been added. The parameters K_0 and K'_0 labeled "acoustic *expt.*" have been measured by ultrasonic experiments at low pressure. The adiabatic to isothermal correction on the acoustic data has been made in Refs. 18 and 20–22.

	V_0 (Å^3)	K_0 (GPa),K'_0 P scale: P_R	K_0 (GPa),K'_0 P scale: P_R	K_0 (GPa), K'_0 RSW-EOS	Ref. RSW-EOS	K_0 (GPa),K'_0 P scale: P'_R	K_0 (GPa),K'_0 P scale: P'_R	K_0 (GPa), K'_0 acoustic expt	Ref. acoustic expt
Au	**16.962**	172.5,5.40 (1.4),(8)	**167**,5.71(3)	**167**,5.82	23	171.0,5.77 (1.4),(8)	**167**,6.00(2)	167,6.2(2)	20
Pt	**15.095**	275.3,4.78 (2.0),(8)	**277**,4.71(2)	**277**,4.66	23	273.6,5.23 (2.0),(8)	**277**,5.08(2)	277	24
Ta	**18.035**	198.2,3.07 (3.1),(14)	**194**,3.25(3)	**194**,3.76	23	197.0,3.39 (3.5),(15)	**194**,3.52(3)	194,3.83(5)	21
W	**15.862**	298.3,3.81 (3.6),(10)	**296**,3.88(2)	**296**,4.45	25	295.2,4.32 (3.9),(11)	**296**,4.30(2)	296–311,4.3	22 and 24
Cu	**11.810**	135.1,4.91 (1.1),(5)	**133**,5.01(1)	**133**,5.33	23	132.4,5.32 (1.4),(6)	**133**,5.30(2)	133,5.4(2)	20 and 26
Al	**16.573**	76.3,4.16 (1.1),(5)	**73**,4.34(2)	**73**,4.50	27	74.3,4.47 (1.1),(6)	**73**,4.54(2)	73,4.42	18

perimental techniques for the determination of the parameters K_0 and K'_0 give more convergent values once the new ruby pressure calibration is used. The remaining differences are not systematic now, and consequently, they can be attributed to the uncertainties of each measurement. The use of the pressure scale proposed by Holzapfel leads to values of fitted K_0 slightly smaller (in average 3 GPa) than when using the current pressure scale. The agreement with ultrasonic K_0 is not better when using Holzapfel's scale, with the Vinet EOS.

In the next section, we compare our EOS data (indicated by expt subscript) obtained using our pressure scale P'_R with EOS calculated by *ab initio* methods.

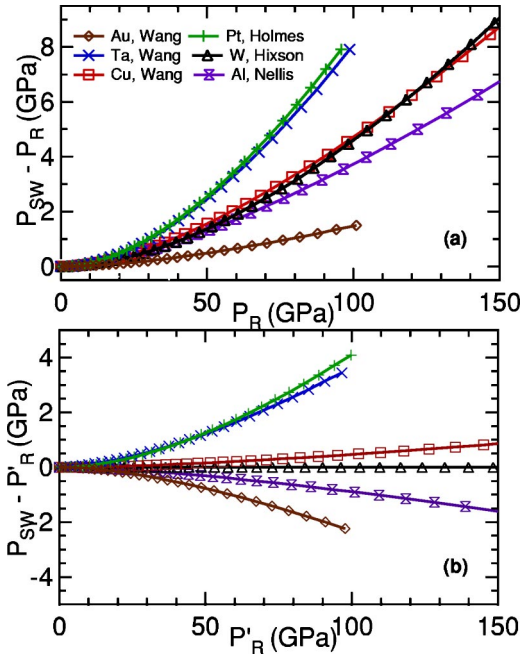

FIG. 3. (a) Difference between reduced shock-wave pressure P_{SW} and static pressure P_R, as a function of P_R at a given atomic volume. P_{SW} and P_R are calculated using Vinet EOS and parameters from Table II: respectively, second, fifth columns and second, fourth columns. (b) Difference between P_{SW} and P'_R (second and seventh-column parameters).

IV. COMPARISON WITH *ab initio* STUDIES

The basic result of DFT-LDA or DFT-GGA electronic calculations is the value of E_C, the 0 K electronic energy, as a function of the atomic volume V of the material. The minimum of the $E_C(V)$ curve corresponds to the equilibrium volume $V_{0\ DFT}$, and its curvature is proportional to bulk modulus $K_{0\ DFT}$. The comparison between experimentals V_0 and K_0 and $V_{0\ DFT}$ and $K_{0\ DFT}$ has thus been used to check the ability of DFT calculations to predict $E_C(V)$ around the equi-

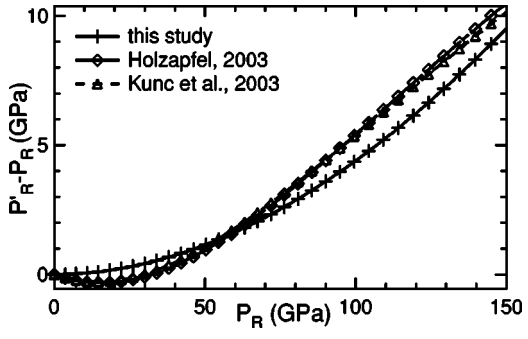

FIG. 4. Differences between new calibrations of the ruby scale and the classical pressure scale proposed by Mao *et al.* (Ref. 6). The crosses correspond to the present calibration, the diamonds to Holzapfel's calibration (Ref. 12), and the triangles to Kunc *et al.*'s calibration (Ref. 13).

TABLE III. Comparison between *ab initio* (subscript *DFT*) and experimental (subscript *expt*) EOS parameters: V_0, K_0, and K_0' are, respectively, volume, incompressibility, and its pressure derivative, at zero pressure. $\Delta V_0=(V_{0\ DFT}-V_{0\ expt})/V_{0\ expt}$.

	$V_{0\ DFT}$ (Å^3)	$V_{0\ expt}$ (Å^3)	ΔV_0 (%)	$K_{0\ DFT}$(GPa), $K'_{0\ DFT}$	$K_{0\ expt}$ (GPa), $K'_{0\ expt}$
Au	17.95[a]	16.962[c]	5.8	132,6.1[a]	167,6.00[c]
Ta	18.36[b]	18.035[c]	1.8	190.3,3.48[b]	194,3.52[c]
W	16.26[b]	15.862[c]	2.5	299.0,4.23[b]	296,4.30[c]
Cu	12.11[b]	11.810[c]	2.5	129.9,5.43[b]	133,5.30[c]
Al	16.75[b]	16.573[c]	1.1	72.6,4.64[b]	73,4.54[c]

[a]From Ref. 40, GGA approximation + spin orbit coupling; thermal pressure and expansion from Ref. 9; *P-V* points fitted with a Vinet EOS between 0 and 150 GPa.
[b]From Ref. 39, GGA approximation; *P-V* points fitted with a Vinet EOS between 0 and 150 GPa.
[c]This study (see Table II).

librium volume.[41,15] It is also interesting to compare experimental and calculated $E_C(V)$ curves, or $P_C(V)=-dE_C/dV$ curves in a large compression range. At ambient temperature, one measures

$$P(V,298\ \mathrm{K}) = P_C(V) + P_{th\ ion}(V,298\ \mathrm{K}) + P_{th\ elec}(V,298\ \mathrm{K}), \tag{2}$$

where $P_{th\ ion}$ and $P_{th\ elec}$ are the thermal pressures, respectively, due to lattice vibrations and thermal excitations of the electrons. In the *P-T* range of interest, $P_{th\ elec}$ is negligible and $P_{th\ ion}$ remains smaller than 2 GPa for the six studied metals. $P(V,298\ \mathrm{K})$ is thus very close to $P_C(V)$. For this reason, ambient pressure EOS are a good test of DFT calculations. However, up to now, the lack of reliable experimental *P-V* data prevented careful comparisons.[42] We believe that the recovered consistency between EOS parameters measured by different techniques, obtained whith the new calibration of the pressure scale, shows that the current data set is now reliable and accurate enough for a meaningful comparison between experimental and calculated $P(V)$ curves.

We have compared the EOS obtained within a given approximation of DFT, the GGA, with our experimental data. Within the GGA, various computational methods should lead to similar EOS, as has been shown in the case of Ta.[14] Consequently, we present here only one set of calculated EOS for each element, published in Ref. 39, for Al, Cu, Ta, and W and in Ref. 40 for Au. To our knowledge, no GGA EOS of Pt is available in the literature.

Table III summarizes the parameters of the experimental and *ab initio* calculated EOS. For calculated EOS, the effect of thermal pressure at 298 K has been taken into account in original work[39] or added using literature data.[9,40] $V_{0\ DFT}$, the equilibrium volume, is seen to be larger by 1.1–5.8% than experimental V_0. Despite this large error on equilibrium volume, K_0 and K_0' predicted by the DFT-GGA are in very good agreement with experimental values (less than 2.3% error on K_0 and 2.5% error for K_0'), except for gold, for which bulk

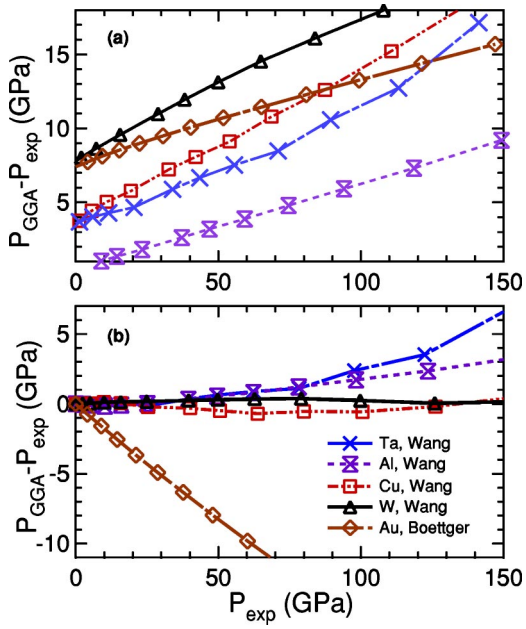

FIG. 5. Difference between *ab initio* GGA pressure and experimental pressure (obtained with the modified ruby scale P_R'), (a) for the same atomic volume V and (b) for the same compression $x=V/V_0$, as a function of experimental pressure, for Al, Cu, Ta, W (Ref. 39), and Au (Ref. 40). The compression is calculated with the reference volume $V_0=V_{0\ expt}$ for P_{expt} and $V_0=V_{0\ DFT}$ for P_{GGA}.

modulus is underestimated by 21%. The differences and similarities between *ab initio* and experimental EOS can also be evidenced by calculating $P_{GGA}-P_{expt}$, for a given atomic volume. In Fig. 5(a), for each metal, $P_{GGA}-P_{expt}$, calculated for a given atomic volume, is plotted as a function of the experimental pressure corresponding to this atomic volume. $P_{GGA}-P_{expt}$ is positive for the scanned pressure range and for all metals studied. This is a direct consequence of the overestimate on the equilibrium volume by GGA calculations: if the volume at zero pressure is overestimated, the pressure necessary to obtain a given volume will also be overestimated. In Fig. 5(a), it also appears that this overestimate increases with increasing pressure. This trend can be simply explained by the incompressibility (i.e., the effect of pressure changes on volume) increase with pressure. At higher pressure, the same ΔV will thus correspond to higher ΔP.

To eliminate this equilibrium volume effect and focus on the effect of compression, we also compared P_{GGA} and P_{expt}, obtained for the same compression—i.e., the same value of V/V_0, V_0 being the ambient pressure volume, calculated (e.g., $V_{0\ DFT}$) for P_{GGA} and measured for P_{expt}. When compared in terms of compression, GGA and experimental EOS of Ta, Cu, W, and Al are in very good agreement, differing by less than 5 GPa at 150 GPa [see Fig. 5(b)]. In other words, the EOS of these four metals can be accurately reproduced by using the experimental V_0 and the calculated K_0 and K_0', which is also evidenced by Table I. This conclusion is similar to the one obtained in the case of diamond by Kunc *et al.*[13] For these metals, the cohesive electronic energy curve $E_C(V/V_0)$ predicted by electronic structure calculations in the GGA is thus very good. However, the comparison is

much less satisfactory for Au. The DFT-GGA calculations largely underestimate the bulk modulus of this metal, which leads to the large discrepancy between P_{GGA} and P_{expt}, as evidenced in Fig. 5(b). This effect is less obvious in Fig. 5(a) because the overestimate of V_0 and the underestimate of K_0 compensate each other in this representation. It has been pointed out that the LDA formulation works better than GGA formulation for this metal,[40] which could be explained by errors compensation.

V. CONCLUSION

In summary, we have shown that using the XRD technique with a third-generation synchrotron source and helium as the pressure transmitting medium, accurate determination of the volume of metals can be extended in the Mbar range. Two main results of the current study can be highlighted: first, the confirmation that the classical ruby pressure scale significantly underestimates the pressure above 1 Mbar. We propose a revision, which keeps the same algebric formulation as the classical ruby scale,[6] and that is in good agreement with pressure scales recently proposed.[12,13] The present calibration is an improvement because it is based on the measured volumes of primary pressure standards over a larger range of pressures and under quasihydrostatic conditions. Second, well-constrained EOS of six metals are obtained. This data set can be reliably used to test the predictions of DFT calculations for the EOS. The parameters K_0 and K_0', calculated within DFT-GGA, are seen to be in good agreement with experiments for Ta, W, Cu, and Al, but surprisingly, a large discrepancy is observed for Au, for which K_0 is underestimated by 21%. Similar measurements should now be performed for more metals, to cover various electronic distributions and understand the reasons of successes and failures of DFT and its approximations. We hope that this project will motivate further experimental and theoretical works.

ACKNOWLEDGMENTS

We acknowledge the European Synchrotron Radiation Facility for provision of synchrotron radiation facilities on beamline ID30. We are grateful to Gunnar Weck for experimental help. We thank Robin Benedetti for reading our manuscript. We thank Carole Bercegeay, Stéphane Bernard, and Gilles Zérah for helpful discussions on DFT calculations.

[1] P. Loubeyre, R. LeToullec, D. Hausermann, M. Hanfland, R. Hemley, H. Mao, and L. Finger, Nature (London) **383**, 702 (1996).
[2] K. Shimizu, K. Suhara, M. Ikumo, M. Eremets, and K. Amaya, Nature (London) **393**, 767 (1998).
[3] R. Boehler, M. Ross, P. Soderlind, and D. B. Boercker, Phys. Rev. Lett. **86**, 5731 (2001).
[4] F. Occelli, P. Loubeyre, and R. Letoullec, Nat. Mater. **2**, 151 (2003).
[5] G. Weck, P. Loubeyre, and R. LeToullec, Phys. Rev. Lett. **88**, 035504 (2002).
[6] H.-K. Mao, J. Xu, and P. Bell, J. Geophys. Res. **91**, 4673 (1986).
[7] F. Datchi, R. LeToullec, and P. Loubeyre, J. Appl. Phys. **81**, 3333 (1997).
[8] N. Holmes, J. Moriarty, G. Gather, and W. Nellis, J. Appl. Phys. **66**, 2962 (1989).
[9] O. Anderson, D. Isaak, and S. Yamamoto, J. Appl. Phys. **65**, 1534 (1989).
[10] H.-K. Mao, P. Bell, J. Shaner, and D. Steinberg, J. Appl. Phys. **49**, 3276 (1978).
[11] C.-S. Zha, H.-K. Mao, and R. Hemley, Proc. Natl. Acad. Sci. U.S.A. **97**, 13494 (2000).
[12] W. Holzapfel, J. Appl. Phys. **93**, 1813 (2003).
[13] K. Kunc, I. Loa, and K. Syassen, Phys. Rev. B **68**, 094107 (2003).
[14] A. Dewaele, P. Loubeyre, and M. Mezouar, Phys. Rev. B **69**, 092106 (2004).
[15] A. Khein, D. J. Singh, and C. J. Umrigar, Phys. Rev. B **51**, 4105 (1995).
[16] A. Hammersley, S. Stevenson, M. Hanfland, A. Fitch, and D. Häusermann, High Press. Res. **14**, 235 (1996).
[17] P. Vinet, J. Ferrante, J. Rose, and J. Smith, J. Geophys. Res. **92**, 9319 (1987).
[18] K. Syassen and W. B. Holzapfel, J. Appl. Phys. **49**, 4427 (1978).
[19] D. E. Gray, *American Institute of Physics Handbook*, 2nd ed. (McGraw-Hill, New York, 1963).
[20] W. Holzapfel, M. Hartwig, and W. Sievers, J. Phys. Chem. Ref. Data **30**, 515 (2001).
[21] K. Katahara, M. Manghnani, and E. Fisher, J. Appl. Phys. **47**, 434 (1976).
[22] D. Steinberg, J. Phys. Chem. Solids **43**, 1173 (1982).
[23] Y. Wang, R. Ahuja, and B. Johansson, J. Appl. Phys. **92**, 6616 (2002).
[24] G. Simmons and H. Wang, *Single Crystal Elastic Constants and Calculated Aggregate Properties: A Handbook* (MIT Press, Cambridge, MA, 1971).
[25] R. Hixson and J. Fritz, J. Appl. Phys. **71**, 1721 (1992).
[26] W. Daniels and C. Smith, Phys. Rev. **111**, 713 (1958).
[27] W. J. Nellis, J. A. Moriarty, A. C. Mitchell, M. Ross, R. G. Dandrea, N. W. Ashcroft, N. C. Holmes, and G. R. Gather, Phys. Rev. Lett. **60**, 1414 (1988).
[28] D. Heinz and R. Jeanloz, J. Appl. Phys. **55**, 885 (1984).
[29] Y. Fei, J. Li, K. Hirose, W. Minarik, J. VanOrman, C. Sanloup, W. VanWestrenen, T. Komabayashi, and K. Funakoshi, Phys. Earth Planet. Inter. **143–144**, 515 (2004).
[30] R. G. Greene, H. Luo, and A. L. Ruoff, Phys. Rev. Lett. **73**, 2075 (1994).
[31] R. J. Hemley, C. S. Zha, A. P. Jephcoat, H. K. Mao, L. W. Finger, and D. E. Cox, Phys. Rev. B **39**, 11 820 (1989).
[32] H. Cynn and C.-S. Yoo, Phys. Rev. B **59**, 8526 (1999).
[33] M. Hanfland, K. Syassen, and J. Köhler, J. Appl. Phys. **91**, 4143 (2002).

[34] R. McQueen, S. Marsh, J. Taylor, J. Fritz, and W. Carter, *High Velocity Impact Phenomenon* (Academic, New York, 1970), Chap. VII.
[35] S. Marsh, *LASL Shock Hugoniot Data* (University of California Press, Berkeley, 1980).
[36] A. Mitchell and W. Nellis, J. Appl. Phys. **52**, 3363 (1981).
[37] J. Morgan, High Temp. - High Press. **6**, 195 (1974).
[38] J. Jamieson, J. Fritz, and M. Manghnani, in *High Pressure Research in Geophysics*, edited by S. Akimoto and M. Manghnani (Center for Academic Publications, Tokyo, 1982), pp. 27-48.
[39] Y. Wang, D. Chen, and X. Zhang, Phys. Rev. Lett. **84**, 3220 (2000).
[40] J. C. Boettger, Phys. Rev. B **67**, 174107 (2003).
[41] V. Ozolins and M. Korling, Phys. Rev. B **48**, 18 304 (1993).
[42] J. C. Boettger, Phys. Rev. B **64**, 035103 (2001).